HHS Public Access

Author manuscript

J Invest Dermatol. Author manuscript; available in PMC 2012 July 01.

Published in final edited form as:

J Invest Dermatol. 2012 January ; 132(1): 198–207. doi:10.1038/jid.2011.248.

Enhanced inflammation and accelerated wound closure following tetraphorbol ester application or full-thickness wounding in mice lacking hyaluronan synthases *Has1* and *Has3*

Judith A. Mack[1,2,5], **Ron J. Feldman**[1,2,5], **Naoki Itano**[3], **Koji Kimata**[4], **Mark Lauer**[1], **Vincent C. Hascall**[1], and **Edward V. Maytin**[1,2,£]

[1]Dept of Biomedical Engineering, Lerner Research Institute, Cleveland Clinic, Cleveland, OH, USA

[2]Dept of Dermatology, Dermatology and Plastic Surgery Institute, Cleveland Clinic, Cleveland, OH

[3]Dept of Molecular Biosciences, Kyoto Sangyo University, Japan

[4]Research Complex for Medicine Frontiers, Aichi Medical University, Aichi, Japan

Abstract

Hyaluronan (HA) is an abundant matrix molecule whose functions in the skin remain to be fully defined. To explore the roles of HA in cutaneous injury responses, double-knockout mice (abbreviated as *Has1/3* null) that lack two HA synthase enzymes (Has1 and Has3) but still express functional Has2, were used in two types of experiments: (i) application of 12-O-tetradecanoylphorbol-13-acetate (TPA), and (ii) full-thickness wounding of the skin. Uninjured *Has1/3* null mice were phenotypically normal. However, after TPA, the accumulation of HA that normally occurs in wildtype epidermis was blunted in *Has1/3* null epidermis. In excisional wound healing experiments, wound closure was significantly faster in *Has1/3* null than in wildtype mice. Coincident with this abnormal wound healing, a marked decrease in epidermal and dermal HA and a marked increase in neutrophil efflux from cutaneous blood vessels were observed in *Has1/3* null skin relative to wildtype skin. *Has1/3* null wounds displayed an earlier onset of myofibroblast differentiation. In summary, selective loss of Has1 and Has3 leads to a pro-inflammatory milieu that favors recruitment of neutrophils and other inflammation-related changes in the dermis.

INTRODUCTION

Hyaluronan (HA) is an abundant extracellular matrix molecule in the dermis and epidermis of skin whose functions are only now beginning to be elucidated. It is a linear, non-sulfated glycosaminoglycan comprised of long chains of disaccharides (N-acetyl-glucosamine and

£**To whom correspondence should be addressed:** Mailstop ND-20, Biomedical Engineering, Cleveland Clinic, 9500 Euclid Avenue Cleveland, OH 44195 Tel: (216) 445-6676 Fax: (216) 444-9198 maytine@ccf.org.

[5]These authors contributed equally to the work.

CONFLICT OF INTEREST: The authors declare no conflict of interest.

glucuronic acid) repeated thousands of times, thereby reaching >10^6 Da in molecular weight (Itano, 2008; Itano *et al*., 1999). In the epidermis, HA is present in the extracellular matrix around keratinocytes (Tammi *et al*., 1988); its rapid turnover rate ($t_{1/2}$ of 1-2 days) (Tammi *et al*., 1991) is determined by a balance between HA degradation (with the exact hyaluronidases responsible still undetermined), and synthesis by three hyaluronan synthases (Has1, Has2, and Has3) that when active reside in the plasma membrane (Rilla *et al*., 2005). The Has enzymes differ in kinetic properties and length of the HA chain produced (Itano *et al*., 1999). HA is normally extruded directly into the extracellular space (Wang and Hascall, 2004). The externalized HA interacts with an HA membrane receptor, CD44, which affects intracellular signaling and thereby regulates cellular proliferation and differentiation (Toole, 2004).

The three Has isoforms and their biological activities have been investigated in gene targeting studies. Functional deletion of the *Has2* gene results in embryonic lethality with severe cardiac and vascular malformations (Camenisch *et al*., 2000). During early embryogenesis, Has2 is responsible for HA production, and loss of Has2 is not compensated for by Has1 or Has3. *Has3* null (knockout) mice on the other hand are viable and fertile, with normal lifespans (Bai *et al*., 2005). *Has1* null mice also appear perfectly normal under non-stressed conditions (Kobayashi *et al*., 2010).

In the skin, all three HAS enzymes are expressed throughout the epidermis and dermis (Sugiyama *et al*., 1998). Current studies suggest that Has3 may be more highly expressed in keratinocytes (Sayo *et al*., 2002), Has1 in fibroblasts (Yamada *et al*., 2004), and Has2 in both cell types. *In vitro* models have been used to evaluate the role of Has enzymes during various perturbations of the epidermis. Treatment of 3-D organotypic keratinocyte cultures with EGF or KGF results in increased proliferation, increased Has2 and Has3 expression, and elevated HA levels (Karvinen *et al*., 2003; Pasonen-Seppanen *et al*., 2003). Physical injury (needle stick) also triggers HA accumulation in the 3-D organotypic keratinocyte cultures, further supporting a causal relationship between inducible Has2 and Has3 expression and increased epidermal HA levels after injury (Monslow *et al*., 2009). Elevated HA levels are often observed in hyperproliferative epidermis in the setting of acute inflammation, so-called inflammatory hyperplasia. Tape-stripping of the skin, a form of physical injury, induces epidermal hyperplasia, inflammatory cell infiltration, transient induction of HA, and elevations in *Has2* and *Has3* mRNA levels (Tammi *et al*., 2005). Skin biopsies from patients with acute eczematous dermatitis (an inflammatory process) demonstrate increased levels of HA in areas of spongiosis, mediated by preferential increases in *Has3* mRNA expression (Ohtani *et al*., 2009). Other evidence also suggests important, complex relationships between the production of HA, leukocyte recruitment, (e.g., gamma/delta T cells) and cytokine production within cutaneous wounds (Jameson *et al*., 2005). Therefore, strong evidence suggests links between the expression of Has enzymes, accumulation of HA, dermal inflammatory cell infiltrates, and epidermal hyperplasia after skin injury. How these events are connected mechanistically, however, remains to be determined.

We utilized two different injury models to elucidate the associations between HA, cutaneous inflammation, and epidermal hyperplasia. The phorbol ester, 12-O-tetradecanoylphorbol-13-

acetate (TPA) is a well-established pro-inflammatory agent that stimulates inflammatory cytokine release, tissue edema, epidermal thickening, and cornified envelope formation when topically applied (Wang and Smart, 1999). TPA-driven inflammatory hyperplasia involves an imbalance between cell cycle stimulation and growth arrest (Marks and Furstenberger, 1993), and protein kinase C (PKC) isoforms are known to be major regulators (Cataisson *et al*., 2005). In studies with PKCα-overexpressing mice harboring an epidermally targeted transgene, TPA application was shown to cause the release of pro-proliferative and chemotactic factors including TNFα, MIP-2, KC, VEGF, and GM-CSF (Cataisson *et al*., 2005). Another type of skin injury that involves cytokine release, inflammation, and epidermal hyperplasia is full-thickness incisional wounding (Singer and Clark, 1999). Wounding triggers recruitment of leukocytes (neutrophils first, followed by macrophages) that have roles in modulating epidermal responses and in regulating the differentiation of fibroblasts into myofibroblasts (Singer and Clark, 1999).

In this paper, we examined possible links between changes in HA accumulation and epidermal and dermal events after skin injury, using a new mouse model that expresses only one of the HA synthetic enzymes, Has2. These mice are nullizygous for *Has1* and *Has3* (abbreviated as *Has1/3* null). In response to skin injury, HA fails to accumulate in *Has1/3* null mice. Using this model, we show that Has1 and Has3 are dispensable for epidermal hyperplasia, but are in fact necessary to properly regulate acute inflammation and fibroblast behavior in the skin following injury.

RESULTS

Mice harboring deletions in the *Has1* gene (Kobayashi *et al*., 2010), or the *Has3* gene (Bai *et al*., 2005) were intercrossed to create *Has1* $^{-/-}$ *Has3* $^{-/-}$ animals (*Has1/3* null). These mice appear grossly normal, with good fertility and normal life spans.

Epidermal induction of HA and CD44 following TPA application is blunted in *Has1/3* null mice

Dorsal skin was treated with TPA, and the skin was examined histologically for changes in morphology, HA, and CD44 (Fig. 1). In wildtype (WT) skin, TPA treatment caused epidermal hyperplasia (compare Fig. 1a and 1d) and a strong epidermal induction of HA, which rose from nearly undetectable levels (Tammi *et al*., 2005) to a very high amount (compare Fig. 1b and 1e). Immunohistochemical analysis of CD44 revealed strongly increased expression after TPA treatment (compare Figs. 1c and 1f). In contrast to WT mice, *Has1/3* null mice showed a blunted response to TPA in terms of epidermal HA levels (compare Figs. 1h and 1k) and CD44 (compare Figs. 1i and 1l). Despite the loss of *Has1* and *Has3*, hyperplastic epidermal thickening in response to TPA still occurred in *Has1/3* null mice, to the same extent as in WT mice (compare Figs. 1g and 1j).

To confirm these findings by an independent method, an ELISA-like assay for HA was utilized (Fig. 1m). When compared to the 6.5-fold increase in HA in WT epidermis (Fig. 1m, left), the 3.6-fold HA induction in *Has1/3* null epidermis was significantly less (Fig. 1m, right).

Epidermal induction of Has enzymes after TPA application in WT and *Has1/3* null mice

To understand the basis for increased HA accumulation after TPA exposure, mRNA expression of HA-synthetic enzymes in the epidermis was examined. Epidermal sheets from vehicle- and TPA-treated WT mouse skin were separated and evaluated by quantitative real-time PCR (Fig. 1n, left). *Has3* mRNA was preferentially increased by 31-fold, *Has2* by 8-fold, *Has1* by 2-fold. In *Has1/3* null epidermis, *Has2* expression after TPA treatment was examined (Fig. 1n, right), and found to be induced to a nearly identical extent (9-fold) as in WT epidermis.

Immunostaining revealed identical expression patterns for markers of keratinocyte proliferation (*Ki67*) and differentiation (keratins *K10* and *K14*) in the WT and *Has1/3* null epidermis (*data not shown*), indicating that *Has1/3* mice mount a normal proliferation and differentiation response to TPA even in the absence of a full HA induction in the epidermis.

Wound healing in *Has1/3* null mice is abnormal, with accelerated wound closure

In a different model of cutaneous injury, full-thickness excisional wounds were generated in WT and *Has1/3* null mice, and the course of wound healing in normal versus null mice was compared (Fig. 2). A striking difference was observed during the first 9 days post-wounding; namely, the rate of wound closure was higher in *Has1/3* null mice than in WT controls (Fig. 2a). Whereas all excisional wounds in mice tended to stretch and expand during the first day after wound placement, *Has1/3* null wounds had returned to the initial 5-mm wound diameter by day 3 and achieved 90% wound closure by day 9. WT wounds did not reach those benchmarks until days 6 and 10, respectively (Fig. 2b). No other major differences were discernable at a macroscopic level.

Both epidermal and dermal levels of HA after skin injury are lower in *Has1/3* null mice, relative to WT mice

We were also interested in evaluating HA in the dermis, in response to TPA and wounding, because dermal HA constitutes the great majority of HA in the skin. To do this, we utilized a biochemical technique called FACE (Fluorophore-Assisted Carbohydrate Electrophoresis) which measures the total mass of HA in tissues (Calabro *et al*., 2000). We measured total HA in WT and *Has1/3* null skin after full-thickness wounding and in TPA treated skin (Fig. 3a, b). In WT mice, full-thickness wounding significantly induces HA levels by 3 days, to ~145% of control levels. While a portion of this increase may reflect increased epidermal HA, as visualized by bHABP staining (Fig. 3c), the bulk of the measured HA accumulation comes from the dermis due to the overwhelming proportion of HA in the dermal compartment. In *Has1/3* null mice, HA levels in control (uninjured) skin were similar to levels in WT controls (Fig. 3a, b). After full-thickness wounding, however, the dermal HA content of *Has1/3* null wounds was significantly less than in WT wounds (Fig. 3a, b), only ~55% the level of uninjured controls. This relative decrease in dermal HA content of *Has1/3* null skin after wounding can also be seen by bHABP staining (Fig. 3c, compare lower left and right panels). Note also that epidermal HA fails to accumulate in *Has1/3* null epidermis (Fig. 3c), as was seen with TPA treatment (Fig. 1).

To determine how changes in *Has* enzyme gene expression might contribute to the changes in overall HA levels after full-thickness injury, a time course experiment using real-time PCR was done to examine *Has* gene expression after wounding in WT and *Has1/3* null mice (Fig. 3d). In WT mice, strong inductions in *Has1* (~100-fold) and *Has3* (~200-fold) were observed at 2-6 h post-wounding. These inductions were transient, declining toward baseline by ~24 h post-wounding. In contrast, *Has2* expression was not induced in WT skin, and in fact declined after 2 h post-wounding. In *Has1/3* null wounds, on the other hand, *Has2* was strongly induced at all times after wounding. However, as shown in Fig. 3a and 3b, this upregulation of *Has2* was not sufficient to compensate for loss of *Has1* and *Has3*, as far as HA induction is concerned.

Increases in TPA-induced inflammation and wound-induced inflammation and fibrosis in *Has1/3* null skin are associated with reduced HA levels

Because we observed a decrease in dermal HA in *Has1/3* null injured skin, and knowing that HA influences inflammation in other systems (Wang *et al*., 2011; Wang and Hascall, 2004), we examined inflammatory responses in our two injury models. After TPA treatment, leukocyte infiltration into the dermis was greater in *Has1/3* null mice than in control mice (Fig. 4a-c), despite the equivalent amounts of epidermal hyperplasia (Fig. 4b and 4c, *double arrows*). This was a mixed inflammatory infiltrate consisting of ~35% neutrophils (determined by comparing H&E stains and neutrophil-specific immunostains using the RB6/85c antibody; *data not show*n). Neutrophils displayed a 3-fold relative increase after TPA in *Has1/3* null mice (Fig. 4j), along with a 5-fold increase in the number of dilated blood vessels in the upper dermis (Fig. 4c, k) suggesting an increased release of vasodilatory cytokines. In full-thickness wounds, a preferential increase in neutrophil recruitment was also seen in the *Has1/3* mice (Fig. 4d, e). During normal wound healing, an influx of neutrophils begins within a few hours after injury and reaches a maximum between days 1 and 3 (Dechert *et al*., 2006). In WT mice at 24 h post-wounding, neutrophils were observed transmigrating from vessels of the subdermal vascular plexus (SVP), a region located immediately beneath the dermis and easily visualized in the skin adjacent to the wound (Fig. 4d; also see the drawings in Figs. 4f, g). In *Has1/3* null mice at 24 h, the number of neutrophils effluxing from the SVP or present in the dermis was markedly increased (Fig. 4e, m, n). This increase in neutrophil recruitment was reflected in the number of intravascular neutrophil aggregates in the SVP that were detected in immunostained sections (Supplem Fig. 1c, c').

Mechanistically, the SVP is of particular interest because this zone appears to contain the highest HA levels of the entire skin (Supplem Fig. 1a) and is a major site of neutrophil recruitment to vessels (Supplem Fig. 1b, b'). Levels of HA in the SVP region are reduced in *Has1/3* null skin, both in the unwounded situation (Supplem Fig. 1a') and at 24 h post-wounding (illustrated in Fig. 4h and 4i, and quantified in Fig. 4L). Notably, double-staining for HA and myeloperoxidase reveals that a robust neutrophil migration from blood vessels in the SVP appears to be significantly associated with low HA in the perivascular matrix (Fig. 4i, m).

A time course experiment provided further evidence that neutrophil recruitment is accelerated in the *Has1/3* null wounds. Whereas more neutrophils were seen at Day 1, fewer were seen at Day 5 (relative to WT wounds), an observation consistent with faster resolution of the neutrophilic infiltrate (Supplem Table 1), although more detailed experiments will be needed to confirm this point. Macrophages, on the other hand, showed similar behavior in the *Has1/3* null and WT wounds, first appearing at Day 3 and becoming equally abundant at Days 5 and 10 (Supplem Table 1).

We also examined the dermal and subcutaneous regions for evidence of relative changes in fibroblast proliferation and differentiation. The results suggest an earlier onset of myofibroblast differentiation in the *Has1/3* null wounds (Supplem Table 1). Beginning at Day 5 after wounding, spindle-shaped cells (many of which expressed alpha-smooth muscle actin; Supplem Fig. 1d, d') appeared in *Has1/3* null skin at the wound edge and beneath the wound bed, but were much less evident in the WT wounds.

DISCUSSION

In this study we examined the epidermal and dermal injury responses in mice lacking *Has1* and *Has3*, as compared to WT mice. Levels of HA, expression of *Has* enzymes, inflammation, and fibroblast behavior were evaluated. Two different kinds of injury, TPA and wounding, were utilized. For both types of injury, similarities in HA responses in the epidermis and in the dermis were noted, as follows. In normal epidermis, large accumulations of HA were observed, both after TPA (Fig. 1e) and after wounding (Fig. 3c). In Has1/3 null epidermis, HA accumulations were smaller than in WT epidermis, but some HA induction was still observed. Levels of CD44 (the HA receptor) on keratinocyte plasma membranes appeared to correlate with overall HA levels (Fig. 1), consistent with suggestions that CD44 levels are controlled by the receptor internalization rate; this rate is slowed when CD44 is retained on the surface through binding to extracellular HA ligand (Knudson *et al*., 2002). In the dermis, changes were more difficult to interpret. In WT skin, dermal HA was increased after wounding (up ~145%) but not after TPA (Fig. 3a, b). In *Has1/3* null skin, on the other hand, either wounding or TPA exposure led to a decline in dermal HA of ~40-50% (Fig. 3b). We can only speculate that this decline is the result of dermal hyaluronidase activity, which becomes unopposed by HA synthesis in mice that lack both Has1 and Has3.

Our data also provide information on the relative contribution that changes in *Has1*, *2*, and *3* expression may be making to the accumulation of HA in epidermal and dermal compartments after injury. Epidermal *Has1* expression remains low (essentially unchanged) after TPA exposure in WT mice (Fig. 1n), suggesting that Has2 and Has3 (which are significantly induced after TPA) are the principal enzymes responsible for HA accumulation in the epidermis following TPA. *Has2* is induced to the same extent in *Has1/3* null epidermis as in WT epidermis (8-fold in each case, Fig. 1n) following TPA injury, which appears to explain why significant amounts of HA can still be synthesized in the *Has1/3* null mice (Fig. 1m). In the dermis, however, both *Has1* and *Has3* are highly induced post-wounding, whereas *Has2* is not. This indicates that Has3 is a major responder following both types of injury, and in both tissue compartments. Interestingly in *Has1/3* null mice, a

compensatory increase in dermal *Has2* expression is observed after wounding as compared to WT mice (Fig. 3d); this could have functional implications, as discussed further below.

Two novel injury phenotypes are observed in *Has1/3* null mice: (i) faster wound closure than in WT mice (Fig. 2), and (ii) an exaggerated neutrophil recruitment following cutaneous injury (Fig. 4). *Has1/3* null wounds were smaller at all time points measured. The enhanced population of myofibrobasts beginning at day 5 in null wounds could account for the faster closure at day 5 and beyond. At earlier time points (days 1 and 3), the lower amounts of HA in *Has1/3* null wounds could lead to drier, less edematous tissue (since HA is very hydrophilic), and hence to a smaller wound size. Alternatively, cytokines released by neutrophils in *Has1/3* null wounds may stimulate premature wound contraction through increased fibroblast cytoskeletal contractility, even in the absence of myofibroblast transformation (Vishwanath *et al*., 2003).

Neutrophils are important participants in a number of inflammatory responses of the skin. In mice, repeated treatment with topical TPA results in a temporal influx of neutrophils that becomes maximal at 3 days (Alford *et al*., 1992). After acute wounding, neutrophil influx into the skin is detectable by 4 hr, and plateaus at ~3 days (Dechert *et al*., 2006; Kim *et al*., 2008). Because the half-life of neutrophils is only a few hours (Kim *et al*., 2008), neutrophil accumulation at wound sites must reflect continuous recruitment of circulating neutrophils, regulated in some manner by HA. In *Has1/3* null mice, reduced levels of dermal HA are associated with an increase in neutrophils at the injury site. In our search for the mechanistic link between HA and enhanced neutrophil recruitment, we hypothesize that reduced HA in *Has1/3* null venular walls (Fig. 4) at sites of injury results in increased neutrophil adhesion. Other studies have shown that HA reduces neutrophil adhesion to human endothelial vein cells *in vitro* (Alam *et al*., 2005; Forrester and Wilkinson, 1981), and that adhesion of neutrophils to postcapillary venules *in vivo* after PMA treatment is inhibited by intravenous administration of HA (Alam *et al*., 2005). An additional hypothesis to explain enhanced neutrophil influx into HA-deficient *Has1/3* null dermis is that HA inhibits neutrophil migration (Alstergren *et al*., 2004). For example, HA-rich tissues (e.g. cartilage; vitreous of the eye) are resistant to influxes of inflammatory cells (Forrester and Lackie, 1981). Other indirect mechanisms may exist. For instance, the synthesis or release of neutrophil chemotactic factors such IL-6 or IL-8 (Pauloin *et al*., 2009) might be altered.

Two additional points of interest can be noted regarding functions of Has enzymes in the skin. *First*, epidermal hyperplasia still occurs in *Has1/3* null mice despite a failure to induce high levels of HA. Therefore, massive epidermal accumulation of HA is not required for epidermal hyperplasia following TPA, but at least some HA may still be needed for proper epidermal proliferation and stratification since Has2 is still expressed in *Has1/3* null epidermis. Partial functional redundancy was described in mice hemizygous for *Has2* and nullizygous for *Has3* (*Has2* +/−, *Has3* −/−) (McDonald and Camenisch, 2002; Spicer *et al*., 2002), suggesting that partial compensation by Has2 is likely in the *Has1/3* null mice. *Secondly*, our data support a role for all three *Has* enzymes in cutaneous responses after injury. In the WT epidermis, mRNA expression of *Has3* and *Has2* was increased more than *Has1* after TPA stimulation (Fig. 1n). In wounded WT whole skin, both *Has1* and *Has3* were induced, whereas *Has2* expression actually declined (Fig. 3d). This suggests that the

relative contribution of different Has enzymes to HA production is dynamic and cell specific, and might contribute to subsequent events through different mechanisms. First, because the average polymer length of HA synthesized by each type of Has enzyme is different (Has1 = Has2 > Has3), a change in the relative amounts of each Has could differentially affect cellular responses. For example, lower mass HA (<200,000 Da), such as that produced by *Has3*, can more efficiently activate intracellular signaling via CD44 (Tammi *et al*., 2002). Second, as mentioned above, different cell types may express distinctly different levels of each Has, leading to different cell-specific responses for keratinocytes, vascular endothelium, and fibroblasts after injury. Other investigators have noted the relative importance of Has3 in keratinocytes under basal conditions (Sayo *et al*., 2002), in response to inflammatory cytokines (Ohtani *et al*., 2009), and during epidermal hyperplasia caused by sonophoresis (Lee *et al*., 2009). TPA can promote phosphorylation of Has3 on a critical serine residue (Goentzel *et al*., 2006), and phosphorylation regulates Has3 activity (Vigetti *et al*., 2009). In mice subjected to ventilator induced lung injury, Has3 was required to generate low MW HA, accompanied by induction of MIP-2 and a neutrophilic infiltrate (Bai *et al*., 2005).

For other tissues, however, Has2 may be of relatively greater importance. In mice, conditional inactivation of *Has2* leads to disruption in mesenchymal (as opposed to epithelial) compartments, including defects in skeletal and cartilage development (Matsumoto *et al*., 2009). In the skin of *Has1/3* null mice, we have shown that *Has2* expression cannot compensate quantitatively for the loss of dermal HA levels. However, the increased *Has2* observed in *Has1/3* null wounds may be contributing to a pro-fibrotic phenotype. Has2 has been implicated in fibrosis following lung injury (Heldin *et al*., 2008), and is thought to have an important role in fibroblast to myofibroblast conversion (Webber *et al*., 2009). Finally, we cannot rule out the possibilty that Has2 induced in *Has1/3* null skin (Fig. 3d) may cause a qualitative change in HA produced at specific locations within the dermis, thus contributing to the pro-inflammatory milieu.

In summary, our study demonstrates that the balance of HA produced by distinct Has enzymes is important for regulating inflammatory responses and wound contraction in the skin after injury. Future studies will address the question of whether altered HA patterns in *Has1/3* null mice can affect long-term scar formation and tensile strength, keeping in mind that faster healing does not necessarily mean better quality healing. Although detailed mechanisms remain to be determined, areas to focus on will be the role of HA in and around venules during neutrophil recruitment, and the role that dermal HA plays in the proliferation and differentiation of myofibroblasts. .

Materials and Methods

Animals

C57BL/6J mice were obtained from JAX Laboratories. *Has1*$^{-/-}$ mice (Kobayashi *et al*., 2010) and *Has3*$^{-/-}$ mice (Bai *et al*., 2005) were generated previously using a strategy that eliminates the catalytic site of each enzyme. *Has1*$^{-/-}$ and *Has3*$^{-/-}$ mice were intercrossed to generate animals nullizygous for both alleles (*Has1/3* null). All mice were maintained in accordance with guidelines of the American Association for the Accreditation of Laboratory

Animal Care, and were approved by our Institutional Animal Care and Use Committee (IACUC).

Injury with 12-o-tetradecanoylphorbol-13-acetate (TPA)

For TPA experiments, dorsal skin of 6-10 wk old mice was shaved 48 h prior to application. TPA (Sigma, St. Louis, MO) was prepared (5 mg, dissolved in 20 ml DMSO and then diluted to 100 ml in acetone) and applied to the animal's back with a cotton swab and gently rubbed (10 μg per application; twice daily for 3 d). Mice were euthanized 2 h after the last treatment, and the skin harvested, fixed in 4% paraformaldehyde, and embedded in paraffin.

Wound healing experiments

All procedures were pre-approval by our institution's Animal Care and Use Committee (IACUC). Mice (C57/BL6 wildtype, or *Has1/3* null, 9-10 weeks of age) were anesthetized with pentobarbital and fur shaved from the upper back. To create full-thickness excisional wounds (one wound per mouse), a 5-mm circular template of sticky tape (cut with a biopsy punch) was placed ~1 cm posterior to the ears. A 5-mm excisional wound created down to fascia, using fine iris scissors. At specified times (from 0 to 11 days), mice were anesthetized with isofluorane and photographed at a fixed distance using a digital camera on a stand. The area of wounds was determined from the digital photos, using image software (pixel counts).

For histological examination, wounds were harvested at 0, 1, 3, 5, and 10 days post-wounding along with unwounded skin. A ~1 cm square of tissue around the wound and beneath the dermis was collected by careful dissection, placed on 3MM Whatman paper (with the orientation noted by marking the caudal pole with a pen). The tissue was bisected with a razor blade oriented in the cephalad-caudad direction. Tissue was fixed in Histochoice (Amresco, Solon, OH), paraffin-embedded, and stored for later sectioning.

Full-thickness linear incisional wounds (1.5 cm long) were made with iris scissors and closed using 6-0 nylon interrupted sutures. Wounds were harvested at 2, 6, 12, and 24 hr post-wounding (2 mm of tissue on either side of the incision). Tissue was frozen and stored at −80 °C for subsequent RNA isolation.

Histology and Immunohistochemistry

Histochoice-fixed or 4% paraformaldehyde-fixed, 5 μm paraffin sections were stained with hematoxylin and eosin using standard methods. For collagen visualization, the Masson Trichrome staining kit (Thermo Fisher Scientific, Pittsburgh, PA) was used according to the manufacturer's protocol. For detection of HA, sections were rehydrated and hyaluronan visualized by immunofluorescence using a biotinylated HA-binding probe (bHABP) and streptavidin-Cy3 (Passi *et al*., 2004). For standard immunohistochemistry, the antibodies and staining conditions are described in Supplemental Materials and Methods.

Quantitation of Hyaluronan by an Enzyme-Linked Immunosorbant Assay (ELISA)-like Assay

Solubilized tissues (either from whole skin adjacent to wounds, or from dispase-separated epidermis) were prepared and analyzed in a competitive ELISA-like assay for HA, modified from Fosang et al. (Fosang *et al*., 1990). Details are provided in Supplemental Materials and Methods.

Quantitation of Hyaluronan by FACE

Fluorophore-assisted carbohydrate electrophoresis (FACE), a technique that quantifies total HA mass, was done as previously described (Calabro *et al*., 2000; Passi *et al*., 2004).

RNA Isolation and qPCR Analysis

RNA was prepared from total skin adjacent to full-thickness incisional wounds, or from dispase-separated epidermis after TPA treatment, then reversed transcribed and subjected to real time quantitative PCR (qPCR) as described in Supplementary Materials and Methods.

Digital image analysis of histological sections

Histological specimens were visualized on an Olympus BX-50 microscope with epifluorescence attachments and a Polaroid DU-DMC2 digital camera. Image processing was done with IPLab Spectrum software as described (Maytin *et al*., 2004).

Statistical Analysis

Differences between experimental and control groups were evaluated with a two-sided Student t-test, assuming equal variance in each group. A P-value of 0.05 or less was considered significant.

Supplementary Material

Refer to Web version on PubMed Central for supplementary material.

ACKNOWLEDGMENTS

We thank Jamie Monslow, PhD for help in developing the qPCR assays. This work was supported in part by grants from NIH/NIAMS grants R01 AR049249 (to EVM) and R56 AR049249 (to EVM), NIH/NHLBI grant P01 HL107147 (to VCH), and from the Women's Dermatologic Society (to RJF).

Abbreviations

bHABP	biotinylated HA-binding protein
ELISA	Enzyme linked immunosorbent assay
FACE	Fluorophore assisted carbohydrate electrophoresis
HA	Hyaluronic Acid
Hyaluronan Has	HA synthase
Hyal	Hyaluronidase

TPA	12-o-tetradecanoylphorbol-13-acetate
WT	wildtype

REFERENCES

Alam CA, Seed MP, Freemantle C, Brown J, Perretti M, Carrier M, et al. The inhibition of neutrophil-endothelial cell adhesion by hyaluronan independent of CD44. Inflammopharmacology. 2005; 12:535–50. [PubMed: 16259720]

Alford JG, Stanley PL, Todderud G, Tramposch KM. Temporal infiltration of leukocyte subsets into mouse skin inflamed with phorbol ester. Agents and Actions. 1992; 37:260–7. [PubMed: 1338267]

Alstergren P, Zhu B, Glogauer M, Mak TW, Ellen RP, Sodek J. Polarization and directed migration of murine neutrophils is dependent on cell surface expression of CD44. Cell Immunol. 2004; 231:146–57. [PubMed: 15919379]

Bai KJ, Spicer AP, Mascarenhas MM, Yu L, Ochoa CD, Garg HG, et al. The role of hyaluronan synthase 3 in ventilator-induced lung injury. Amer J Resp Crit Care Med. 2005; 172:92–8. [PubMed: 15790861]

Calabro A, Benavides M, Tammi M, Hascall VC, Midura RJ. Microanalysis of enzyme digests of hyaluronan and chondroitin/dermatan sulfate by fluorophore-assisted carbohydrate electrophoresis (FACE). Glycobiology. 2000; 10:273–81. [PubMed: 10704526]

Camenisch TD, Spicer AP, Brehm-Gibson T, Biesterfeldt J, Augustine ML, Calabro A Jr. et al. Disruption of hyaluronan synthase-2 abrogates normal cardiac morphogenesis and hyaluronan-mediated transformation of epithelium to mesenchyme. J Clin Invest. 2000; 106:349–60. [PubMed: 10930438]

Cataisson C, Pearson AJ, Torgerson S, Nedospasov SA, Yuspa SH. Protein kinase C alpha-mediated chemotaxis of neutrophils requires NF-kappa B activity but is independent of TNF alpha signaling in mouse skin in vivo. J Immunol. 2005; 174:1686–92. [PubMed: 15661932]

Dechert TA, Ducale AE, Ward SI, Yager DR. Hyaluronan in human acute and chronic dermal wounds. Wound Repair Regen. 2006; 14:252–8. [PubMed: 16808803]

Forrester JV, Lackie JM. Effect of hyaluronic acid on neutrophil adhesion. J Cell Sci. 1981; 50:329–44. [PubMed: 7320071]

Forrester JV, Wilkinson PC. Inhibition of leukocyte locomotion by hyaluronic acid. J Cell Sci. 1981; 48:315–31. [PubMed: 7276093]

Fosang AJ, Hey NJ, Carney SL, Hardingham TE. An ELISA plate-based assay for hyaluronan using biotinylated proteoglycan G1 domain (HA-binding region). Matrix. 1990; 10:306–13. [PubMed: 2150688]

Goentzel BJ, Weigel PH, Steinberg RA. Recombinant human hyaluronan synthase 3 is phosphorylated in mammalian cells. Biochem J. 2006; 396:347–54. [PubMed: 16522194]

Heldin P, Karousou E, Bernert B, Porsch H, Nishitsuka K, Skandalis SS. Importance of hyaluronan-CD44 interactions in inflammation and tumorigenesis. Connective Tiss Res. 2008; 49:215–8.

Itano N. Simple primary structure, complex turnover regulation, and multiple roles of hyaluronan. J Biochem. 2008; 144:131–7. [PubMed: 18390876]

Itano N, Sawai T, Yoshida M, Lenas P, Yamada Y, Imagawa M, et al. Three isoforms of mammalian hyaluronan synthases have distinct enzymatic properties. J Biol Chem. 1999; 274:25085–92. [PubMed: 10455188]

Jameson JM, Cauvi G, Sharp LL, Witherden DA, Havran WL. Gammadelta T cell-induced hyaluronan production by epithelial cells regulates inflammation. J Exper Med. 2005; 201:1269–79. [PubMed: 15837812]

Karvinen S, Pasonen-Seppanen S, Hyttinen JM, Pienimaki JP, Torronen K, Jokela TA, et al. Keratinocyte growth factor stimulates migration and hyaluronan synthesis in the epidermis by activation of keratinocyte hyaluronan synthases 2 and 3. J Biol Chem. 2003; 278:49495–504. [PubMed: 14506240]

Kim MH, Liu W, Borjesson DL, Curry FR, Miller LS, Cheung AL, et al. Dynamics of neutrophil infiltration during cutaneous wound healing and infection using fluorescence imaging. J Invest Dermatol. 2008; 128:1812–20. [PubMed: 18185533]

Knudson W, Chow G, Knudson CB. CD44-mediated uptake and degradation of hyaluronan. Matrix Biol. 2002; 21:15–23. [PubMed: 11827788]

Kobayashi N, Miyoshi S, Mikami T, Koyama H, Kitazawa M, Takeoka M, et al. Hyaluronan deficiency in tumor stroma impairs macrophage trafficking and tumor neovascularization. Cancer Res. 2010; 70:7073–83. [PubMed: 20823158]

Lee SE, Jun JE, Choi EH, Ahn SK, Lee SH. Stimulation of epidermal calcium gradient loss increases the expression of hyaluronan and CD44 in mouse skin. Clin Exper Dermatol. 2009; 35:650–7. [PubMed: 19886962]

Marks F, Furstenberger G. Proliferative responses of the skin to external stimuli. Environ Health Perspect. 1993; 101(Suppl 5):95–101. [PubMed: 8013432]

Matsumoto K, Li Y, Jakuba C, Sugiyama Y, Sayo T, Okuno M, et al. Conditional inactivation of Has2 reveals a crucial role for hyaluronan in skeletal growth, patterning, chondrocyte maturation and joint formation in the developing limb. Development. 2009; 136:2825–35. [PubMed: 19633173]

Maytin EV, Chung HH, Seetharaman VM. Hyaluronan participates in the epidermal response to disruption of the permeability barrier in vivo. American J Pathol. 2004; 165:1331–41.

McDonald JA, Camenisch TD. Hyaluronan: genetic insights into the complex biology of a simple polysaccharide. Glycoconjugate J. 2002; 19:331–9.

Monslow J, Sato N, Mack JA, Maytin EV. Wounding-induced synthesis of hyaluronic acid in organotypic epidermal cultures requires the release of heparin-binding egf and activation of the EGFR. J Invest Dermatol. 2009; 129:2046–58. [PubMed: 19225541]

Ohtani T, Memezawa A, Okuyama R, Sayo T, Sugiyama Y, Inoue S, et al. Increased hyaluronan production and decreased E-cadherin expression by cytokine-stimulated keratinocytes lead to spongiosis formation. J Invest Dermatol. 2009; 129:1412–20. [PubMed: 19122650]

Pasonen-Seppanen S, Karvinen S, Torronen K, Hyttinen JM, Jokela T, Lammi MJ, et al. EGF upregulates, whereas TGF-beta downregulates, the hyaluronan synthases Has2 and Has3 in organotypic keratinocyte cultures: correlations with epidermal proliferation and differentiation. J Invest Dermatol. 2003; 120:1038–44. [PubMed: 12787132]

Passi A, Sadeghi P, Kawamura H, Anand S, Sato N, White LE, et al. Hyaluronan suppresses epidermal differentiation in organotypic cultures of rat keratinocytes. Exper Cell Res. 2004; 296:123–34. [PubMed: 15149843]

Pauloin T, Dutot M, Liang H, Chavinier E, Warnet JM, Rat P. Corneal protection with highmolecular-weight hyaluronan against in vitro and in vivo sodium lauryl sulfate-induced toxic effects. Cornea. 2009; 28:1032–41. [PubMed: 19724206]

Rilla K, Siiskonen H, Spicer AP, Hyttinen JM, Tammi MI, Tammi RH. Plasma membrane residence of hyaluronan synthase is coupled to its enzymatic activity. J Biol Chem. 2005; 280:31890–7. [PubMed: 16014622]

Sayo T, Sugiyama Y, Takahashi Y, Ozawa N, Sakai S, Ishikawa O, et al. Hyaluronan synthase 3 regulates hyaluronan synthesis in cultured human keratinocytes. J Invest Dermatol. 2002; 118:43–8. [PubMed: 11851874]

Schmittgen TD, Livak KJ. Analyzing real-time PCR data by the comparative C(T) method. Nat Protoc. 2008; 3:1101–8. [PubMed: 18546601]

Singer AJ, Clark RAF. Cutaneous wound healing. New Engl J Med. 1999; 341:738–46. [PubMed: 10471461]

Spicer AP, Tien JL, Joo A, Bowling RA. Investigation of hyaluronan function in the mouse through targeted mutagenesis. Glycoconjugate J. 2002; 19:341–5.

Sugiyama Y, Shimada A, Sayo T, Sakai S, Inoue S. Putative hyaluronan synthase mRNA are expressed in mouse skin and TGF-beta upregulates their expression in cultured human skin cells. J Invest Dermatol. 1998; 110:116–21. [PubMed: 9457904]

Tammi MI, Day AJ, Turley EA. Hyaluronan and homeostasis: a balancing act. J Biol Chem. 2002; 277:4581–4. [PubMed: 11717316]

Tammi R, Pasonen-Seppanen S, Kolehmainen E, Tammi M. Hyaluronan synthase induction and hyaluronan accumulation in mouse epidermis following skin injury. J Invest Dermatol. 2005; 124:898–905. [PubMed: 15854028]

Tammi R, Ripellino JA, Margolis RU, Tammi M. Localization of epidermal hyaluronic acid using the hyaluronate binding region of cartilage proteoglycan as a specific probe. J Invest Dermatol. 1988; 90:412–4. [PubMed: 2450149]

Tammi R, Saamanen AM, Maibach HI, Tammi M. Degradation of newly synthesized high molecular mass hyaluronan in the epidermal and dermal compartments of human skin in organ culture. J Invest Dermatol. 1991; 97:126–30. [PubMed: 2056182]

Toole BP. Hyaluronan: from extracellular glue to pericellular cue. Nat Rev Cancer. 2004; 4:528–39. [PubMed: 15229478]

Vigetti D, Genasetti A, Karousou E, Viola M, Clerici M, Bartolini B, et al. Modulation of hyaluronan synthase activity in cellular membrane fractions. J Biol Chem. 2009; 284:30684–94. [PubMed: 19737932]

Vishwanath M, Ma L, Otey CA, Jester JV, Petroll WM. Modulation of corneal fibroblast contractility within fibrillar collagen matrices. Invest Ophthalmol Vis Sci. 2003; 44:4724–35. [PubMed: 14578392]

Wang A, de la Motte C, Lauer M, Hascall V. Hyaluronan matrices in pathobiological processes. FEBS J. 2011 E-pub ahead of print, Epub date 2011/03/03.

Wang A, Hascall VC. Hyaluronan structures synthesized by rat mesangial cells in response to hyperglycemia induce monocyte adhesion. J Biol Chem. 2004; 279:10279–85. [PubMed: 14679194]

Wang HQ, Smart RC. Overexpression of protein kinase C-alpha in the epidermis of transgenic mice results in striking alterations in phorbol ester-induced inflammation and COX-2, MIP-2 and TNF-alpha expression but not tumor promotion. J Cell Sci. 1999; 112(Pt 20):3497–506. [PubMed: 10504298]

Webber J, Meran S, Steadman R, Phillips A. Hyaluronan orchestrates transforming growth factor-beta1-dependent maintenance of myofibroblast phenotype. J Biol Chem. 2009; 284:9083–92. [PubMed: 19193641]

Yamada Y, Itano N, Hata K, Ueda M, Kimata K. Differential regulation by IL-1beta and EGF of expression of three different hyaluronan synthases in oral mucosal epithelial cells and fibroblasts and dermal fibroblasts: quantitative analysis using real-time RT-PCR. J Invest Dermatol. 2004; 122:631–9. [PubMed: 15086545]

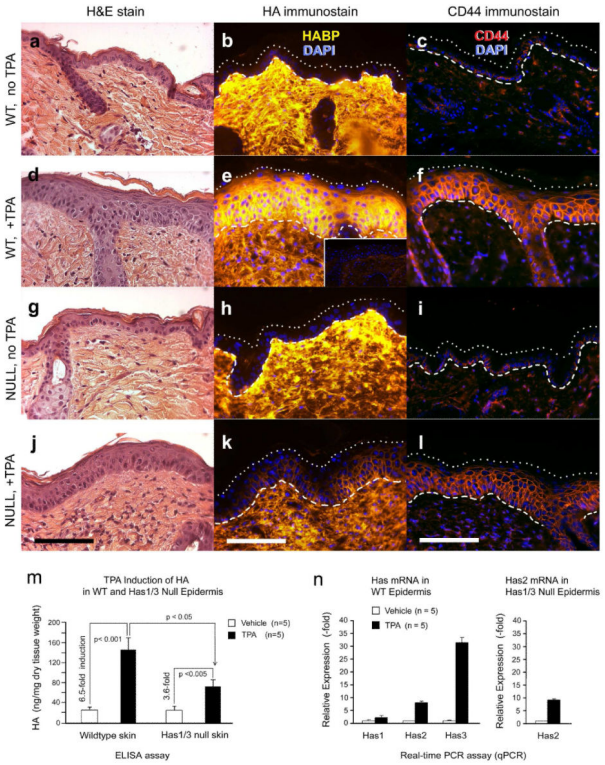

Figure. 1. TPA-stimulated accumulation of HA in the epidermis is blunted in *Has1/3* null mice

(***a-l***) Dorsal skin was treated with TPA or vehicle alone (x 3 days), biopsied, and evaluated histologically for morphologic changes (H&E stains), HA levels (bHABP and streptavidin-Cy3), and CD44 protein levels (anti-CD44/rhodamine). Specific HA staining was confirmed by pretreatment of specimens with hyaluronidase (**panel e**, *Inset*). (***m, n***) TPA-treated or control epidermis was separated using dispase, and analyzed for concentrations (ng/mg) of HA using an ELISA-like assay (***m***), or analyzed for relative expression of *Has1*, *Has2*, and *Has3* mRNA using quantitative real-time PCR (qPCR) (***n***). In *Has1/3* null skin, only *Has2* expression was analyzed. The p values from two-sided Student t-test are indicated. *Dashed/dotted lines:* epidermal boundaries. Scale bars, 100 μm.

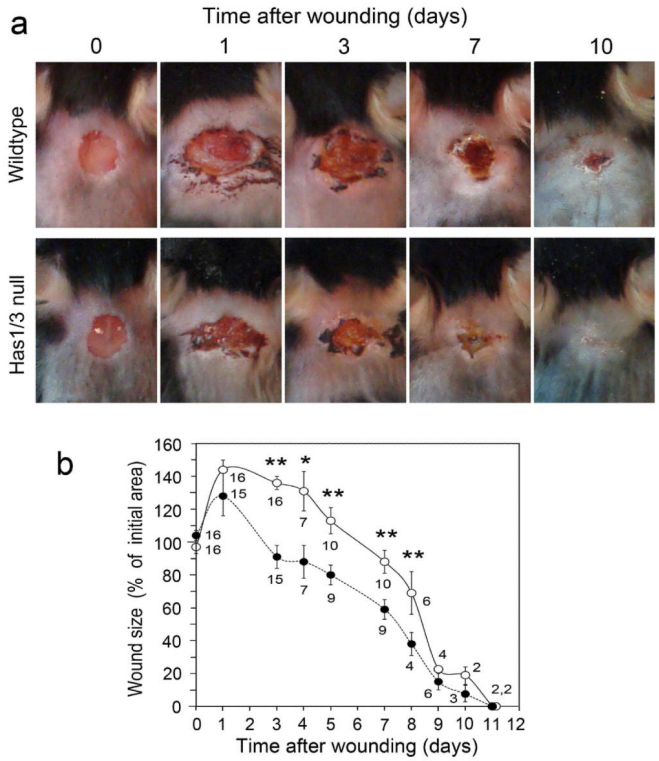

Figure 2. Wound closure is accelerated in *Has1/3* null mice

(a) Typical examples of 5-mm diameter full-thickness excisional wounds. Wounds were photographed daily until closure. (**b**) Graphical summary of changes in wound area, expressed relative to the initial size of the wound at day zero. Data are mean ± SEM; the number of mice analyzed at each time point is shown beneath each data symbol. *Open circles*, wildtype; *Closed circles*, *Has1/3* null. (*), $p < 0.01$; (**), $p < 0.005$ by two-sided Student t-test.

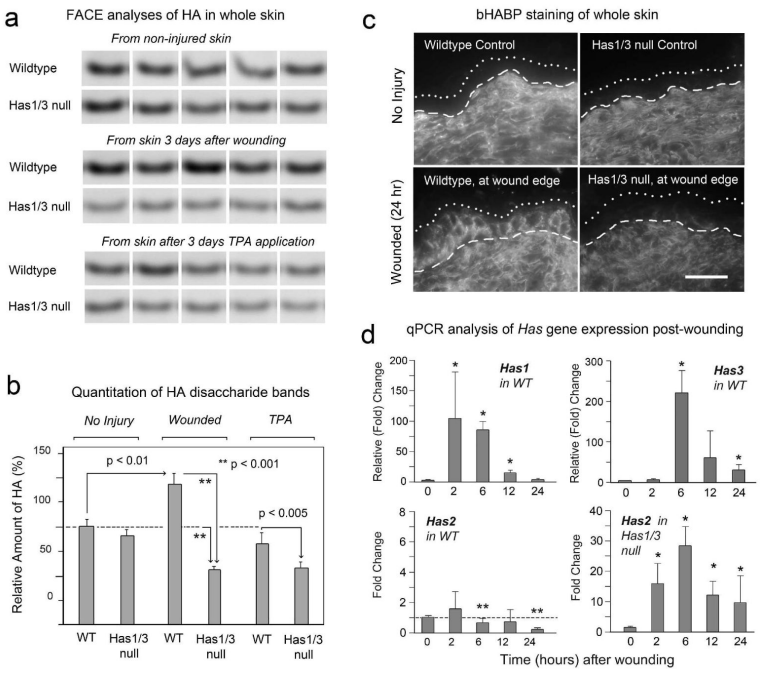

Figure 3. HA levels are altered in *Has1/3* null mice after wounding

(a) Fluorescence-Assisted Carbohydrate Electrophoresis analysis of HA levels in equivalent amounts (weight) of skin from WT or *Has1/3* null mice; treatments as shown. Disaccharide (Δ di-HA) bands are displayed for individual wounds (5 mice/condition). (**b**) Integrated fluorescent intensity of Δ di-HA bands from 3-day wounds or TPA-treated skin, relative to WT non-injured controls (mean ± SD, n=5). (**c**) HA in skin adjacent to incisional wounds (<1 mm from wound edge) at 24 h post-injury, immunostained with bHABP/streptavidin-Cy3. *Bar*, 25 μm. (**d**) Time course of Has mRNA expression post-wounding in WT mice or *Has1/3* null mice. Mean ± SD, duplicate mice, triplicate qPCR reactions per wound. (*) significant increase or (**) significant decrease, at $p<0.05$ level.

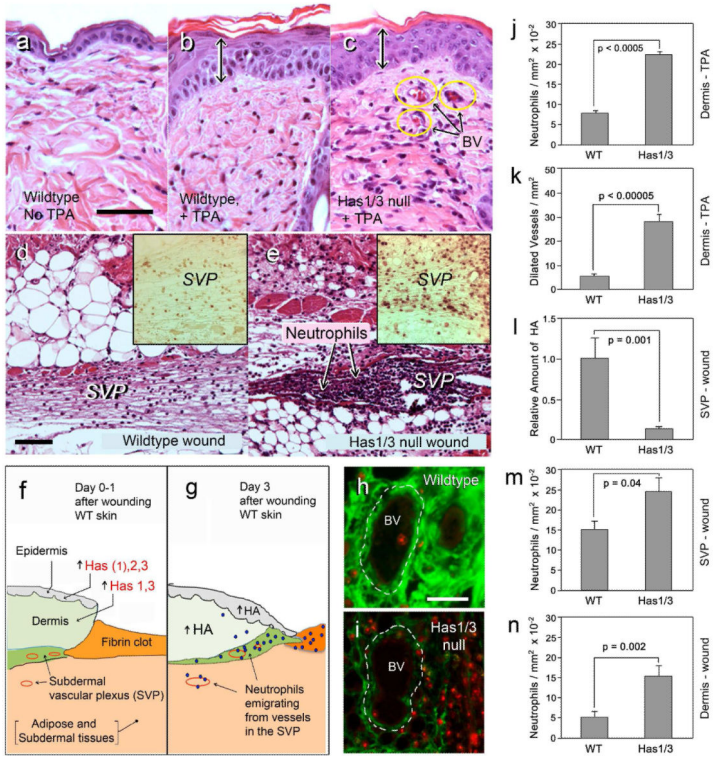

Figure 4. Preferentially enhanced inflammation in *Has1/3* null skin following TPA application (3 days) or full-thickness wounding (24 hours)

(a-c) H&E stains of non-injured wildtype, TPA-treated wildtype, or TPA-treated *Has1/3* null skin. *BV*, dilated blood vessels. **(d, e)** Masson-Trichrome stains of subdermal vascular plexus (*SVP*) immediately adjacent to the wound, in wildtype or *Has1/3* null mice. *Insets*, neutrophil-specific immunostains of the SVP. (***f***, ***g***): Cartoon of events in wildtype skin after wounding. (***h***, ***i***) Tissues in the SVP region, co-stained for HA (green) and neutrophils (red). GRAPHS: Data (mean ± SEM) for neutrophils (***j***) and dilated vessels (***k***) after TPA treatment; or HA staining intensity (***l***), neutrophils near blood vessels in the subdermis (***m***), and neutrophils in the dermis (***n***) of wounded skin. Scale bars, 50 μm.